Theoretical determination of the effective velocity parameter in atomic and molecular scattering from surfaces

W. W. Hayes and J. R. Manson
Department of Physics and Astronomy, Clemson University, Clemson, South Carolina 29634, USA
(Received 30 April 2006; published 31 August 2006)

A useful theoretical expression for interpreting and analyzing observed scattering intensity spectra for atomic and molecular collisions with surfaces is the differential reflection coefficient for a smooth, vibrating surface. This differential reflection coefficient depends on a parameter, usually expressed in dimensions of velocity, that arises due to correlated motions of neighboring regions of the surface and can be evaluated if the polarization vectors of the phonons near the surface are known. In this paper experimental conditions are suggested under which this velocity parameter may be more readily evaluated than it has been in the past.

DOI: 10.1103/PhysRevB.74.073413 PACS number(s): 34.50.Dy, 34.50.Pi, 82.20.Rp

The scattering of atomic and molecular particles has proven to be a useful method for obtaining a wide variety of information on the structure and dynamics of surfaces. In many cases such experiments are carried out under classical conditions involving a combination of large incident energies, heavy atomic masses, and high surface temperatures, conditions for which large numbers of phonons are transferred in the collision process. In the classical scattering limit, two closed-form expressions for the differential reflection coefficient have been shown to be useful in explaining observed distributions of scattered particles, which typically consist of both total angular distributions and energy-resolved intensity spectra taken at fixed incident and final angles. The first of these expressions, called the discrete model, assumes that the incoming projectile collides with a surface of discrete atoms having an equilibrium distribution of thermal energies and whose vibrational motions are uncorrelated. Its differential reflection coefficient $dR(\mathbf{p}_f,\mathbf{p}_i)/d\Omega_f dE_f$, which expresses the fractional probability per unit final energy E_f and per unit final solid angle $d\Omega_f$ of a beam of particles initially prepared with well defined momentum $\mathbf{p}_i$ making a transition to momentum state $\mathbf{p}_f$ after a single collision, is (Refs. 1–3)

$$\frac{dR(\mathbf{p}_f,\mathbf{p}_i)}{d\Omega_f dE_f} = \frac{m^2|\mathbf{p}_f|}{8\pi^3\hbar^4 p_{iz}}|\tau_{fi}|^2\left(\frac{\pi}{k_B T_S \Delta E_0}\right)^{1/2} \times \exp\left\{-\frac{(E_f - E_i + \Delta E_0)^2}{4k_B T_S \Delta E_0}\right\}, \quad (1)$$

where p_{iz} is the surface normal component of $\mathbf{p}_i$, T_S is the surface temperature, k_B is Boltzmann's constant, the recoil energy is $\Delta E_0 = (\mathbf{p}_f - \mathbf{p}_i)^2/2M_C$ with M_C the surface atomic mass, and $|\tau_{fi}|^2$ is a form factor that depends on the interaction potential. If $|\tau_{fi}|^2$ is chosen to be a constant, the value appropriate for hard sphere scattering, then Eq. (1) contains no undefined parameters.

The second of these two expressions, called the smooth surface model, describes scattering from a potential which is on average flat but has vibrationally induced corrugations due to the thermal motions of the underlying atoms. Its differential reflection coefficient is given by (Refs. 3–6)

$$\frac{dR(\mathbf{p}_f,\mathbf{p}_i)}{d\Omega_f dE_f} = \frac{m^2 v_R^2|\mathbf{p}_f|}{8\pi^3\hbar^2 p_{iz} S_{u.c.}}|\tau_{fi}|^2\left(\frac{\pi}{k_B T_S \Delta E_0}\right)^{3/2} \times \exp\left\{-\frac{(E_f - E_i + \Delta E_0)^2 + 2v_R^2\mathbf{P}^2}{4k_B T_S \Delta E_0}\right\}, \quad (2)$$

where S_{uc} is the area of a surface unit cell and $\mathbf{P}$ is the projection of the scattering momentum $\mathbf{p_f} - \mathbf{p_i}$ parallel to the surface. The difference with respect to Eq. (1) is the appearance of an additional Gaussian-like factor in parallel momentum transfer $\mathbf{P}$ and the envelope prefactor varies as the power 3/2 instead of 1/2. This behavior is due to the effects of correlations in vibrations of closely neighboring parts of the surface and as a result of the fact that the law of conservation of momentum applies only to components parallel to the surface.

Both Eq. (1) and (2) have been shown to explain certain types of experiments. The discrete model of Eq. (1), with the form factor $|\tau_{fi}|^2$ taken as a constant has been shown to explain the shape as well as the temperature and energy dependence of the single scattering peak observed in the collisions of low energy ions with metal surfaces.[7,8] It has also been useful for describing energy-resolved spectra for heavy rare gas scattering from molten metal surfaces.[9,10] The smooth surface model of Eq. (2) explains the temperature and incident energy dependence of He atom scattering from a metal surface at high temperatures and energies,[11,12] and describes the angular distributions and energy-resolved spectra observed in rare gas scattering from liquid metals and metal alloys.[9,10,13]

The smooth surface model depends on a parameter v_R usually expressed in dimensions of velocity which is a weighted average of all phonon speeds at the surface. It can be expressed in terms of the surface phonon polarization vectors at the classical turning point, and for highly symmetric crystals has the form (Refs. 4 and 5)

$$\frac{1}{v_R^2} = \frac{1}{2k_B T_S \mathbf{k}^2}\sum_{\mathbf{Q}}\sum_{\nu}\frac{\hbar\mathbf{Q}^2}{N\omega_\nu(\mathbf{Q})}|\mathbf{k}\cdot\mathbf{e}(\mathbf{Q},\nu)|^2[2n(\omega_\nu(\mathbf{Q})) + 1], \quad (3)$$

where the scattering wave vector is $\mathbf{k} = (\mathbf{p}_f - \mathbf{p}_i)/m$, $\omega_\nu(\mathbf{Q})$ is the frequency of a phonon mode with parallel wave vector $\mathbf{Q}$

and perpendicular index ν, N is the number of modes, $n(\omega)$ is the Bose-Einstein occupation number, and $\mathbf{e}(\mathbf{Q},\nu)$ is the polarization vector of the $(\mathbf{Q},\nu)$ phonon mode. Although v_R is completely defined through Eq. (3) if the phonon spectral density is known, it is usually treated as an adjustable parameter for fitting calculations of the differential reflection coefficient of Eq. (2) to experimental data.[4–6]

The typical experiments for which Eqs. (1) and (2) have been useful are scattering of beams of the heavy rare gas atoms. The measured energy-resolved intensity spectra for fixed incident and scattering angles usually consist of a single broad peak whose width increases and whose maximum intensity decreases with increasing incident temperature. The measurements are usually made at angles that maximize the intensity observed in the peak. Under such conditions, calculations using Eqs. (1) and (2) will produce peaks with maxima located at close to the same energy positions (i.e., located at nearly the same most probable final energies) but Eq. (1) gives peaks that are typically broader in energy width than those observed experimentally. Eq. (2), because it contains an additional Gaussian-like term in the parallel momentum transfer $\mathbf{P}$ will produce a peak with an increasingly narrow energy width as v_R is increased and the value of v_R is usually chosen by matching the width of the scattered distribution to that of the experimental data.

The object of this paper is to suggest a different set of experimental conditions under which the parameter v_R can be more accurately extracted from the energy-resolved spectra. This suggestion is to compare calculations with data taken at angles that differ from maximum intensity conditions, because at such angles there will be a difference between predictions of Eqs. (1) and (2) for the most probable energy position of the peak and that energy shift will be strongly dependent on v_R.

An example is shown in Fig. 1 which gives calculations for Ar with an incident energy of E_i=40 kJ/mol (415 meV) scattered from a liquid In surface at a temperature of 436 K, slightly higher than its melting point. The incident angle is θ_i=46° and the final angle is θ_f=44° corresponding to a fixed source-to-detector angle θ_{SD}=90° which is a commonly found experimental geometry. The dashed curve is the calculation of the discrete model of Eq. (1) and the solid curve is the calculation of the smooth surface model of Eq. (2) and there is a clear shift in energy denoted by δE_{mp} between their most probable energy positions. This shift is a function of v_R which in this case is chosen to be 2000 m/s.

The origin of the δE_{mp} shift between the two calculations is the Gaussian-like term in $\mathbf{P}$ appearing in the smooth surface model. For the discrete model of Eq. (1) the most probable energy position is very nearly given by the condition that the argument of the exponential vanishes, i.e., $E_f - E_i + \Delta E_0 = 0$. This condition is equivalent to the well-known Baule relation $E_f = f(\mu,\theta)E_i$ for the final energy as a function of total scattering angle θ for an elastic collision between an incoming particle of mass m and energy E_i and a stationary particle with mass M_C. The function $f(\mu,\theta)$ is determined by the conditions of conservation of energy and momentum and depends on mass ratio $\mu = m/M_C$ and total scattering angle (θ is the angle between $\mathbf{p}_f$ and $\mathbf{p}_i$).

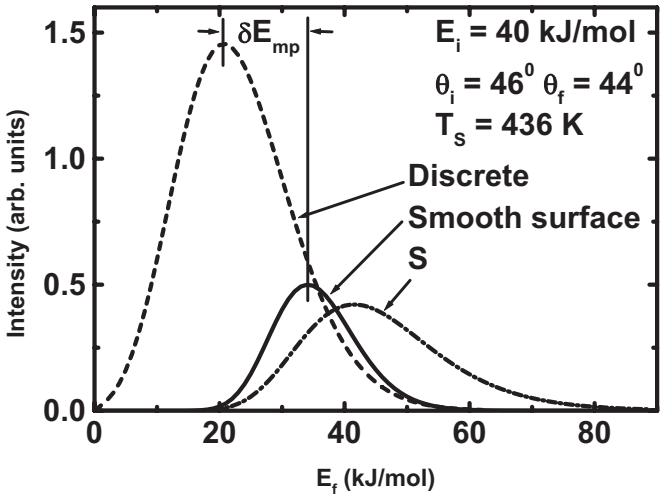

FIG. 1. Calculated energy resolved intensity spectra of Ar scattered from In for E_i=40 kJ/mol and T_S=436 K. The solid curve is the smooth-surface calculation of Eq. (2) for θ_i=46° and θ_f=90°−θ_i=44° and v_R=2000 m/s, conditions corresponding to 50% of the maximum of the most probable intensity at the critical angle as shown in more detail in Fig. 2. The dashed curve is the discrete model calculation of Eq. (1), and the dash-dotted curve is the function $S(\mathbf{p}_f,\mathbf{p}_i)$ of Eq. (4).

For a given incident and final angle the most probable intensity of the smooth surface model of Eq. (2) occurs near the energy that minimizes the argument of the exponential. However, only at certain angles will this minimum argument actually vanish, because this requires the simultaneous conditions of $E_f - E_i + \Delta E_0 = 0$ and $\mathbf{P}=0$. Close to these critical angles of most probable energy the most probable intensity will tend to achieve local maximum values. For example, under the initial conditions of Fig. 1 this occurs at the angle $\theta_i \approx 37°$ (and consequently $\theta_f \approx 53°$). Another way of describing the smooth surface model is to view it as the product of the discrete model differential reflection coefficient multiplied by the following Gaussian-like function in parallel momentum transfer:

$$S(\mathbf{p}_f,\mathbf{p}_i) = |\tau'_{fi}|^2 \left(\frac{\pi}{k_B T_S \Delta E_0}\right) \exp\left\{-\frac{2v_R^2 \mathbf{P}^2}{4k_B T_S \Delta E_0}\right\}. \quad (4)$$

The function $S(\mathbf{p}_f,\mathbf{p}_i)$ is also plotted in Fig. 1 with the matrix element given by

$$\tau'_{fi} = 4p_{fz}p_{iz}/m, \quad (5)$$

the Jackson-Mott matrix element taken in the limit for a strongly repulsive barrier, an approximate form that has been very useful in the analysis of atomic and molecular scattering data.[10,13]

It is now clear from Fig. 1 that the energy-resolved spectrum of the smooth surface model can be viewed as the product of Eq. (1) for the discrete model and the Gaussian-like function of Eq. (4) in parallel momentum $\mathbf{P}$. The resulting product is also roughly Gaussian in shape and of similar width, but its intensity is substantially reduced with respect to that of the discrete model and its most probable energy is

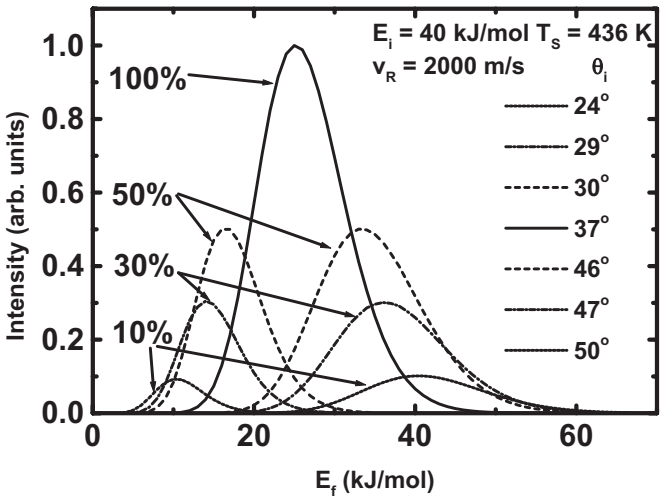

FIG. 2. Energy resolved spectra of Ar scattered from In for T_S =436 K and E_i=40 kJ/mol with a fixed θ_{SD}=90°. Critical angular conditions for a maximum of the most probable scattered intensity occur at θ_i=37° as indicated by a solid curve. Pairs of other curves are drawn for angular conditions at which the most probable intensity is 50, 30, and 10% of this maximum, as marked. In each pair, the smaller angle corresponds to the peak shifted to lower energy than that for θ_i=37°.

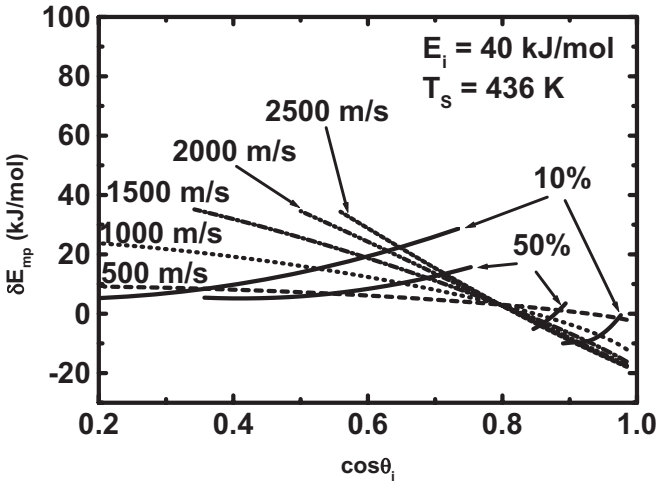

FIG. 3. The energy shift δE_{mp} vs cos θ_i for the same conditions as in Fig. 2, calculated for several different values of v_R as indicated. The solid curves are the loci of points for which the most probable scattering intensity is 50, and 10%, respectively, of the maximum most probable intensity.

shifted. The suggestion of this paper is that comparing this energy shift δE_{mp} with experimental measurements taken at a wide range of scattering angles will be a much more sensitive way of choosing the parameter v_R than simply fitting the shape of the curve for the energy-resolved intensity spectrum in the region of angles where that spectrum is maximized. This suggestion will also be applicable to determining the scaling parameter of other theories of surface scattering that contain product Gaussian functions of parallel momentum transfer.[14]

As implied above, most experimental studies of energy-resolved spectra have been carried out with incident and detection angles adjusted near the critical conditions of maximum intensity, which closely corresponds to the positions where the argument of the exponential of Eq. (2) vanishes. The calculations presented in Fig. 1 show that when the observation conditions deviate from those optimal critical angles the intensity strongly decreases. This effect, in fact, has been indirectly noted in measurements of angular distributions,[15,16] both those measured with fixed incident angle and those measured by varying the incident angle in a detector with a fixed source-detector angle θ_{SD}.[17,18] For both types of angular distributions, calculations using the discrete model predict scattered distributions that have full widths at half maximum that are much too broad. In contrast, the smooth surface model with an appropriate choice of the parameter v_R gives a good fit to the observed scattered angular distributions.[10,19,20]

Because the observable intensity decreases rapidly as incident and detector angles deviate from the optimum angles, this gives rise to the question of whether there will be sufficient intensity to measure when the energy shift δE_{mp} becomes appreciable. This question is addressed in Fig. 2 which is carried out for the same incident conditions as Fig. 1 with a fixed θ_{SD}=90° and v_R=2000 m/s. The solid curve shows the predictions of the smooth surface model at the critical maximum intensity angle θ_i=37°. The two long-dashed curves, one on each side of the solid curve, show calculations for incident angles at which the predicted intensity is 50% of the maximum. One of these two peaks, for θ_i=46°, is the same calculation shown in Fig. 1 where it is clear that the energy shift is $\delta E_{mp} \approx 14$ kJ/mol or about a third of the incident energy. Two further pairs of curves are given in Fig. 2 that show calculations for incident angles at which the predicted most probable intensity is 30 and 10% of the maximum. For these latter curves the energy shift δE_{mp} is even larger, as large as one third of the incident energy for the 10% case. Thus, the calculations in Fig. 2 imply that substantial energy shifts can be obtained while still retaining sufficient intensity for measurement.

The question of expected energy shift dependency on incident angle and on the parameter v_R is addressed in Fig. 3. This shows, for the same incident conditions as in Fig. 2 and with θ_{SD}=90°, calculations of δE_{mp} as a function of cos θ_i for several selected values of v_R. For small values of v_R the energy shifts are not large, but for v_R as large as 2000 m/s the energy shift can become comparable to the incident energy. Note that at the critical point of maximum intensity, at cos θ_i=0.8 for this case, there is a small energy shift between the two calculations due to the different prefactors in Eqs. (1) and (2). Also shown in Fig. 3 are a pair of solid curves, one on either side of the critical angle, marked 50% and another similar pair marked 10%. These two pairs of curves mark the locus of points where the most probable intensity predicted by the smooth surface model is 50 and 10%, respectively, of the maximum value at the critical angle. Thus, if at least 50% of the maximum observable intensity is required for measurements, this calculation implies that measurements can be made for all angles between the two solid curves labeled 50%. These calculations indicate that energy shifts as large as 20 kJ/mol, or up to half the incident energy in this case,

can in principle be measured. Such sizeable shifts, together with the prediction that the corresponding intensities are readily observable, would indicate that rather precise values of v_R could be obtained by fitting data to the smooth surface theory.

The smooth surface theory of Eq. (2) has proven to be quite useful in the interpretation and analysis of data for atom and molecule scattering from surfaces, but it does depend on the velocity parameter v_R. However, precise knowledge of v_R can be important because it provides physical information on the system dynamics, in particular it can be related to the polarization vectors of the phonons at the classical turning point through its defining Eq. (3). In the past, the method of determining the parameter v_R has been to measure energy-resolved intensity spectra at angles close to conditions that maximize the observed intensities, and then fit Eq. (2) to the width of the observed experimental peak using v_R as a variable parameter. In this paper it is suggested that a much more precise way of determining v_R is to make measurements over a range of incident and final angles that deviate from the critical conditions of maximum intensity, and then determine v_R by fitting the energy shifts δE_{mp} with respect to the parameter-free discrete model predictions of Eq. (1). Calculations for a wide range of systems and initial conditions, of which specific examples are shown here, indicate that such measurements should be feasible.

ACKNOWLEDGMENTS

This work was supported by the DOE under Grant No. DE-FG02-98ER45704.

[1] A. Sjölander, Ark. Fys. **14**, 315 (1959).
[2] D. Micha, J. Chem. Phys. **74**, 2054 (1981).
[3] J. R. Manson, Phys. Rev. B **43**, 6924 (1991).
[4] R. Brako and D. M. Newns, Phys. Rev. Lett. **48**, 1859 (1982).
[5] R. Brako, Surf. Sci. **123**, 439 (1982).
[6] H.-D. Meyer and R. D. Levine, Chem. Phys. **85**, 189 (1984).
[7] A. Muis and J. R. Manson, Phys. Rev. B **54**, 2205 (1996).
[8] J. Powers, J. R. Manson, C. E. Sosolik, J. R. Hampton, A. C. Lavery, and B. H. Cooper, Phys. Rev. B **70**, 115413 (2004).
[9] A. Muis and J. R. Manson, J. Chem. Phys. **107**, 1655 (1997).
[10] A. Muis and J. R. Manson, J. Chem. Phys. **111**, 730 (1999).
[11] M. Bertino and J. R. Manson, J. Chem. Phys. **108**, 10239 (1998).
[12] F. Hoffman, J. P. Toennies, and J. R. Manson, J. Chem. Phys. **106**, 1234 (1997).
[13] J. Dai and J. R. Manson, J. Chem. Phys. **119**, 9842 (2003).
[14] V. Celli, G. Benedek, U. Harten, J. P. Toennies, R. B. Doak, and V. Bortolani, Surf. Sci. **143**, 376 (1984).
[15] Warren R. Ronk, Daniel V. Kowalski, Michelle Manning, and Gilbert M. Nathanson, J. Chem. Phys. **104**, 4842 (1996).
[16] M. Manning, J. A. Morgan, D. J. Castro, and G. M. Nathanson, J. Chem. Phys. **119**, 12593 (2003).
[17] T. Tomii, T. Kondo, T. Hiraoka, T. Ikeuchi, S. Yagu, and S. Yamamoto, J. Chem. Phys. **112**, 9052 (2000).
[18] T. Kondo, T. Sasaki, and S. Yamamoto, J. Chem. Phys. **118**, 760 (2003).
[19] Iryna Moroz and J. R. Manson, Phys. Rev. B **69**, 205406 (2004).
[20] Iryna Moroz and J. R. Manson, Phys. Rev. B **71**, 113405 (2005).